Science Bulletin 66 (2021) 1698–1704

Contents lists available at ScienceDirect

Science Bulletin

journal homepage: www.elsevier.com/locate/scib

Article

Carbon turnover times shape topsoil carbon difference between Tibetan Plateau and Arctic tundra

Donghai Wu [a,1], Dan Liu [b,1], Tao Wang [b,c], Jinzhi Ding [b], Yujie He [d], Philippe Ciais [e], Gengxin Zhang [b,*], Shilong Piao [a,b,c,*]

[a] Sino-French Institute for Earth System Science, College of Urban and Environmental Sciences, Peking University, Beijing 100871, China
[b] Key Laboratory of Alpine Ecology, Institute of Tibetan Plateau Research, Chinese Academy of Sciences, Beijing 100085, China
[c] Center for Excellence in Tibetan Plateau Earth Sciences, Chinese Academy of Sciences, Beijing 100085, China
[d] Department of Earth System Science, University of California, Irvine, CA 92697, USA
[e] Laboratoire des Sciences du Climat et de l'Environnement, LSCE/IPSL, CEA-CNRS-UVSQ, Université Paris-Saclay, F-91191 Gif-sur-Yvette, France

ARTICLE INFO

Article history:
Received 14 December 2020
Received in revised form 17 March 2021
Accepted 18 March 2021
Available online 1 May 2021

Keywords:
Tibetan Plateau
Arctic tundra
Soil organic carbon
Net primary production
Carbon turnover time
Radiocarbon

ABSTRACT

The Tibetan Plateau (TP) and Arctic permafrost constitute two large reservoirs of organic carbon, but processes which control carbon accumulation within the surface soil layer of these areas would differ due to the interplay of climate, soil and vegetation type. Here, we synthesized currently available soil carbon data to show that mean organic carbon density in the topsoil (0–10 cm) in TP grassland (3.12 ± 0.52 kg C m^{-2}) is less than half of that in Arctic tundra (6.70 ± 1.94 kg C m^{-2}). Such difference is primarily attributed to their difference in radiocarbon-inferred soil carbon turnover times (547 years for TP grassland versus 1609 years for Arctic tundra) rather than to their marginal difference in topsoil carbon inputs. Our findings highlight the importance of improving regional-specific soil carbon turnover and its controlling mechanisms across permafrost affected zones in ecosystem models to fully represent carbon-climate feedback.

1. Introduction

The thawing of carbon-rich permafrost could cause a positive feedback to climate change due to enhanced carbon decomposition rate with global warming [1,2]. The importance of permafrost to climate change is determined in part by the size of the soil carbon pool, with a higher soil carbon content generally generating a larger impact. Due to rapid climate warming and its amplification in permafrost areas, ~5%–15% of the permafrost carbon is vulnerable to thawing, and subsequently likely to return to the atmosphere by the end of this century [3].

The world's "Third Pole", Tibetan Plateau (TP), is the largest permafrost affected zones aside from the Arctic regions. However, according to all available evidence, the soil organic carbon densities exhibit large difference between the two regions [4,5]. Currently, there is still a lack of understanding in the formation of different soil carbon densities within the surface active layer of soil which acts as an essential interface between the vegetation and the underlying permafrost. It is well established that net soil carbon accumulation is a long-term balance between carbon gains through litter production and carbon losses through organic carbon decomposition [6,7]. There is also clear evidence to show that TP grassland differs from Arctic tundra in terms of temperature, solar insolation, topography and the degree of vegetation coverage [8]. Such differences could lead to different environmental constraints on the processes which affect the variations of regional soil carbon density. Thus, a critical question is how the processes control soil carbon difference between TP grassland and Arctic tundra. Resolving this issue could provide new model formulations for describing soil carbon accumulation processes in different permafrost affected zones, which should, in turn, help to improve our current understanding of the carbon-climate feedback.

In this study, we first assessed the difference of topsoil organic carbon density (0–10 cm) between TP grassland and Arctic tundra with multi-source datasets. To understand how the difference of topsoil organic carbon density between the two regions was formed, we then investigated the main drivers of soil organic carbon in terms of carbon inputs and carbon turnover times [7,9]. Furthermore, we explored the possible mechanisms of the difference in soil carbon turnover times between the two regions.

* Corresponding authors.
E-mail addresses: zhangg@itpcas.ac.cn (G. Zhang), slpiao@pku.edu.cn (S. Piao).
[1] These authors contributed equally to this work.

https://doi.org/10.1016/j.scib.2021.04.019
2095-9273/

2. Materials and methods

2.1. Study regions

We used the grassland type in the International Geosphere-Biosphere Programme (IGBP) classification provided by the land cover product (MCD12C1) from Moderate Resolution Imaging Spectroradiometer (MODIS) [10] to define the grassland areas on the TP (Fig. S1a online). Arctic tundra was defined as a combination of grassland and open shrubland north of 55°N [11], but excluded peatlands (histel and histosol landcover classes with > 15% coverage) [5] which have different soil carbon dynamics (Fig. S1b online).

2.2. Soil organic carbon density (SOCD)

The topsoil organic carbon density (0–10 cm) in TP grassland and Arctic tundra was estimated from three observation-based data sources (Figs. S2 and S3 online). The first soil carbon dataset is the latest SoilGrids database [12]. The SOCD was reported for six intervals (0–5, 5–15, 15–30, 30–60, 60–100 and 100–200 cm). For the SoilGrids dataset that provides SOCD for different soil layers, we simply calculated the topsoil (0–10 cm) organic carbon density as

$$\mathrm{SOCD}_{0-10\ \mathrm{cm}} = \mathrm{SOCD}_{0-5\ \mathrm{cm}} + 0.5\mathrm{SOCD}_{5-15\ \mathrm{cm}}. \quad (1)$$

Second, we used the World Inventory of Soil Property Estimates (WISE) dataset [13] which is an up-to-date global soil carbon dataset based on approximately 21,000 soil profiles and geographical data. The third dataset is the soil carbon map combining the Harmonized World Soil Database (HWSD) and the Northern Circumpolar Soil Carbon Database (NCSCD) [5,14]. Because both datasets provide SOCD with 1 m depth, we fitted a relationship between cumulative proportion of SOCD (equal to 0.0 at 0 cm depth, and 1.0 at 100 cm depth) and soil depth to derive the topsoil organic carbon density:

$$y = a\ln(bx + 1), \quad (2)$$

where x is the soil depth (cm), y is the cumulative proportion of SOCD, and a and b are fitted parameters. The data used for fitting the parameters are multi-site average cumulative proportion of SOCD for different soil layers in TP grassland and Arctic tundra, respectively [15–17]. The fitted functions are: y = 0.397ln (0.122x + 1) (R^2 = 0.99, N = 7) for TP grassland; and y = 0.494ln (0.073x + 1) (R^2 = 0.98, N = 6) for Arctic tundra (Fig. S4 online). The calculated proportions of accumulated SOCD for 0–10 cm against 0–100 cm soil layers are estimated to be 0.316 for TP grassland and 0.271 for Arctic tundra.

2.3. Primary productivity

We used two gross primary productivity (GPP) datasets that were both extrapolated from site-level eddy flux measurements by a machine learning algorithm (model tree ensemble, MTE). The first GPP dataset is from Jung et al. [18] which upscaled eddy-covariance observations of CO_2 fluxes to the global scale using MTE. This dataset spans the period from 1982 to 2011 with a spatial resolution of 0.5°×0.5°. The second dataset is derived from Yao et al. [19], and has improved estimates of GPP over China with eddy flux measurements from 40 sites, especially for the data-limited TP grassland. Here, we used GPP data from Jung et al. [18] for Arctic tundra and the GPP data from Yao et al. [19] for TP grassland, which show high quality for representing the gross photosynthesis of the two regions (Fig. S5 online).

We used net primary productivity (NPP) as a proxy for potential soil carbon inputs, given that total litter production should be approximately equal to NPP over herbaceous ecosystems under the steady state assumption. To estimate the NPP, we multiplied MTE-derived GPP by a spatial explicit estimate of the carbon use efficiency at a spatial resolution of 1°. The spatially variable carbon use efficiency is produced by combing a diagnostic ecosystem carbon balance model (DALEC2) with satellite observations and soil carbon dataset [20] (Fig. S6 online). NPP was further separated into aboveground NPP (ANPP) and belowground NPP (BNPP), which consisted of BNPP in the top 10 cm of soil and BNPP deeper than 10 cm depth. First, we estimated aboveground biomass (AGB) from normalized difference vegetation index (NDVI) using AGB = $a \times \mathrm{NDVI}^b$ [21]. In TP grassland, the relationship between NDVI and AGB is AGB (g C m^{-2}) = 65.987 × $\mathrm{NDVI}^{0.8841}$ (R^2 = 0.61, N = 115) [22] (Fig. S7 online). In the Arctic tundra, we used the relationship: AGB (g C m^{-2}) = 393.73 × $\mathrm{NDVI}^{1.3256}$ (R^2 = 0.92, N = 11) [23] (Fig. S8a online). The NDVI data for each field observation of AGB was extracted from a maximum annual NDVI dataset using GIMMS NDVI at a spatial resolution of 1/12° for the year during which the biomass was collected [24]. Here, the AGB maps were created using multi-year mean annual maximum NDVI for the period 1982–2011. We next estimated regional ANPP from AGB. In TP grassland, ANPP is taken to be equal to AGB by assuming that the longevity of the aboveground parts of the grassland is one year [21]. For Arctic tundra, we estimated ANPP from AGB based on the equation ANPP (g C m^{-2} a^{-1}) = 0.0983 × $\mathrm{AGB}^{1.1425}$ (R^2 = 0.85, N = 87) [25] (Fig. S8b online). The BNPP was obtained by subtracting ANPP from NPP. Here, we calculated BNPP in the layers above and below a depth of 10 cm by using the vertical distributions of roots. This distribution was characterized as $Y = 1 - \beta^d$, where Y is cumulative percentage of root biomass from the soil surface to the depth d (cm), and β is the fitted parameter derived from field observations [26]. In the TP grassland, β is 0.937 for alpine steppe and 0.900 for alpine meadow [26], and β is 0.914 for Arctic tundra [27]. In this study, the sum of ANPP and BNPP in the 0–10 cm layer is used as a proxy for potential topsoil carbon inputs via litter fall to the surface layer (Figs. S9 and S10 online).

2.4. Environmental data

Mean annual temperature (MAT), mean annual precipitation (MAP) and mean annual solar radiation (MAR) are taken from the WorldClim Version 2.0 dataset, which is averaged for the years 1970–2000 at a spatial resolution of ~1 km (Figs. S11–S13 online) [28]. Altitude data (elevation above sea level, m) is from the WorldClim Version 1.4 dataset (Fig. S11 online). The ultraviolet-B (UV-B) radiation dataset, which has a spatial resolution of 15 arc-minutes and covers the period 2004–2013, was used (Fig. S13 online) [29]. The SoilGrids database provides global soil texture at specific soil depths (0, 5, 15, 30, 60, 100 and 200 cm) [12], and we therefore use the texture at the depth of 5 cm (middle of 0–10 cm layer) to represent the topsoil texture [12] (Fig. S14 online).

2.5. Soil carbon turnover time

The technique, based on the radioactive decay of ^{14}C originating from atmospheric testing of nuclear weapons [30], provides information on the turnover times of C atoms in the soil reservoir. Here, we used 21 soil profiles with radiocarbon measurements (^{14}C) from the TP grassland (Fig. S1 online). 17 of the 21 profiles were sampled in 2012 and 2010, and fraction modern (F) of ^{14}C for topsoil (0–10 cm) was measured at the accelerator mass spectrometry laboratory of Beta Analytic. The remaining 4 profiles were sampled in 2003 at Haibei Station, in the northeast TP, and were collated from Tao et al. [31]. For Arctic tundra, we assembled 10 soil profiles that had ^{14}C measurements for the 0–10 cm layer from He et al. [32]. These profiles were sampled during 1986 and 2011. In addi-

tion, to compare the carbon turnover times from the two cold ecosystems with those from other ecosystems, we compiled a global ^{14}C dataset, using 106 topsoil ^{14}C measurements from different ecosystems at the global scale [32,33]. These ^{14}C observations were then converted into soil carbon turnover times for all sites, using box model forced with ^{14}C measurements and past atmospheric ^{14}C records under the assumption that the topsoil layer is a homogeneous reservoir [34]. In a general form, this numerical approximation is given by

$$(F^{'}C)_{t+1} = (F^{'}C)_t + \partial(F^{'}C)_t, \quad (3)$$

where $F^{'}$, the absolute fraction modern, refers to the absolute ratio of sample to standard, corrected for radioactive decay in the year of measurement. $(F^{'}C)_t$ represents the ^{14}C content at time t and $(F^{'}C)_{t+1}$ represents the ^{14}C content at time $t + 1$. $\partial(F^{'}C)_t$ represents the differential of ^{14}C content. The difference approximation can be derived using Euler's method [34]:

$$F^{'}_{t+1}C_{t+1} = IF^{'}_{\mathrm{atm},t} + F^{'}_t C_t(1 - k - \lambda), \quad (4)$$

where $F^{'}_{\mathrm{atm},t}$ is the absolute fraction modern in the atmosphere at a given time t; k represents the rate of carbon decomposition; λ is the radioactive decay constant (1/8267 a^{-1}). When we treat the soil system as a steady state system, $C_{t+1} = C_t$ and $I = kC$, and so eq. (4) can be rearranged as

$$F^{'}_{t+1} = kF^{'}_{\mathrm{atm},t} + F^{'}_t(1 - k - \lambda). \quad (5)$$

Eq. (5) allows us to create an iterative computer program to determine the optimized k with the use of past atmospheric ^{14}C records (50 ka BP–2012) [32,35,36]. The carbon turnover time of the measured soil sample is given by $1/k$.

3. Results and discussion

3.1. Topsoil carbon density

Given the large uncertainties in gridded SOC databases, we used the three different sources of datasets to estimate SOCD in the top 10 cm for TP grassland and Arctic tundra (Figs. 1, S2, and S3 online). The SOCD varies between 2.52 kg C m^{-2} from HWSD and 3.43 kg C m^{-2} from SoilGrids. The SOCD discrepancy among datasets is larger in Arctic tundra, with SOCD varying between 5.18 kg C m^{-2} from WISE and 8.88 kg C m^{-2} from SoilGrids. On grid scale, the SOCD generally increases from western to eastern TP. In Arctic tundra, SOCD in Eurasia is larger than that in Northern America (Fig. S2 online). In spite of uncertainties in the gridded SOC dataset, the SOCD in the top 10 cm layer over TP grassland (3.12 ± 0.52 kg C m^{-2}) is less than half of that in Arctic tundra (6.70 ± 1.94 kg C m^{-2}), and this result is found in all the three datasets.

3.2. Topsoil carbon inputs

The annual MTE-based NPP (multi-year mean for the period 1982–2011) is 149 g C m^{-2} a^{-1} over TP grassland and 164 g C m^{-2} a^{-1} over Arctic tundra (Figs. 1, S9, and S10 online). The magnitude is also comparable to DALEC2 NPP (127 g C m^{-2} a^{-1} for TP grassland and 158 g C m^{-2} a^{-1} for Arctic tundra, Figs. S15 and S16 online). At the spatial scale, higher NPP is observed in eastern than in western regions of TP grassland, and that in Eurasia than in Northern America of Arctic tundra. After separating MTE-based NPP into ANPP and BNPP for two soil layers (0–10 cm and > 10 cm; see Materials and methods), the sum of ANPP and BNPP in the 0–10 cm layer was then used as a proxy for potential topsoil carbon inputs via litter fall to the surface layer. Our results show that sum of ANPP and BNPP in the 0–10 cm layer is similar between TP grassland (100 g C m^{-2} a^{-1}) and Arctic tundra (116 g C m^{-2} a^{-1}) (Figs. 1, S9, and S10 online). In addition, we also separated the DALEC2 NPP using similar decomposition methods (Figs. S15 and S16 online), suggesting that the magnitude of potential carbon input (sum of ANPP and BNPP in the 0–10 cm layer) is also comparable between TP grassland (87 g C m^{-2} a^{-1}) and Arctic tundra (112 g C m^{-2} a^{-1}). Therefore, the results imply that soil carbon inputs alone could not explain the more than twofold difference in SOCD between the two regions (Fig. 1).

Here we used the sum of ANPP and BNPP in the 0–10 cm layer as a proxy for litter fall to represent the topsoil carbon inputs. Nevertheless, it should be noted that litter fall only represents a potential carbon source to soil carbon pool rather than the actual carbon influx, since a part of the litter fall is respired back to the atmosphere during litter fragmentation [37]. Recent review suggested that the carbon use efficiency from plant litter to SOC is about 6.6% for aboveground inputs and 39% for belowground inputs in agricultural field [37]. However, estimation of the actual soil carbon influx still needs more field or laboratory experiments of isotopically labelled little decomposition in the permafrost regions in future work [38].

3.3. Topsoil carbon turnover time

We then quantified soil carbon turnover time with a box model using radiocarbon (^{14}C) measurements in topsoil (see Materials and methods). The results showed that the turnover times in the TP grassland and Arctic tundra (403^{1176}_{113} years, $N = 31$, for 90 percent confidence interval) are significantly higher than other ecosystems in the world (120^{835}_{50} years, $N = 106$) (Figs. S17 and S18 online), suggesting much slower SOC decomposition rates in these cold ecosystems. Furthermore, the mean topsoil soil carbon turnover times across TP grassland and Arctic tundra sites are 338^{893}_{112} years ($N = 21$, where the subscripts and superscripts represent 90% confidence intervals) and 611^{1696}_{149} years ($N = 10$), respectively. Using regression analysis, we found that the turnover time covaried significantly ($R^2 = 0.44$) with mean annual temperature (MAT) but relatively weaker relationship ($R^2 = 0.23$) with mean annual precipitation (MAP) in Arctic tundra. By contrast, there is a significant spatial correlation between the turnover time and MAP ($R^2 = 0.23$) in TP grassland (Fig. 2). Although the relationship between turnover time and MAT is relatively weaker in TP grassland ($R^2 = 0.13$), the turnover time showed robust relationship with altitude ($R^2 = 0.49$) (Fig. S19 online). Negative correlations between turnover time and temperature in both regions are linked to an expected increase in microbial decomposition with temperature [39]. We observed that higher precipitation is strongly associated with a shorter turnover time in TP grassland, indicating that moisture effects also determined the decomposition process.

To estimate the turnover time at the regional level, we upscaled the soil carbon turnover time from sites to regions based on environmental controls of turnover time across sites. To do this, we built a predictive model of turnover time by linking the logarithm of the turnover time with environmental factors using multiple linear regression. Optimum relationships were detected for the TP grassland and Arctic tundra as follows, TP: ln(SOC-turnover time) = 0.0006altitude − 0.0020MAP + 4.0813; Arctic: ln(SOC-turnover time) = − 0.1961MAT + 0.0026MAP + 4.3257. The resulting model had a relatively high predictive power, with 57.4% of the total spatial variance of the turnover time explained by MAP and altitude in TP grassland, and 56.6% by MAT and MAP in Arctic tundra. Our cross-validation approach also allows us to generate a spatially explicit understanding of model uncertainties in the two regions. Across all pixels, we found that soil carbon turnover times gradually become shorter from western to eastern regions in TP

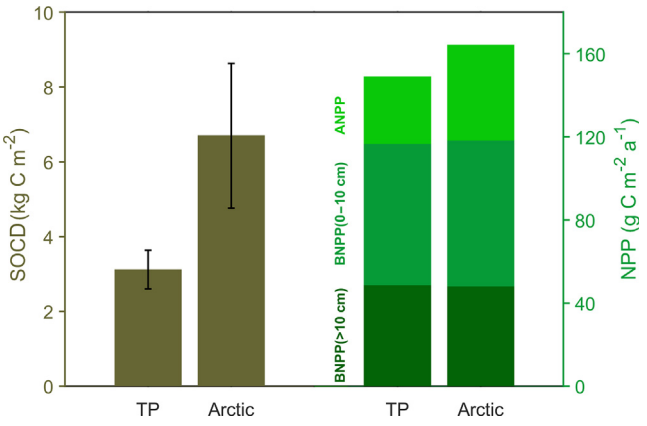

Fig. 1. Soil organic carbon density (SOCD) and net primary production (NPP) in Tibetan Plateau (TP) grassland and Arctic tundra. Here, soil organic carbon density in the top 10 cm was derived from three observation-based databases. The NPP represents the multi-year mean for the period 1982–2011. NPP was separated into aboveground NPP (ANPP) and belowground NPP (BNPP), which consisted of BNPP in the 0–10 cm layer and BNPP at depths >10 cm. The sum of ANPP and BNPP in the 0–10 cm layer is used as a proxy for potential topsoil carbon inputs via litter fall to the surface layer based on the steady state assumption.

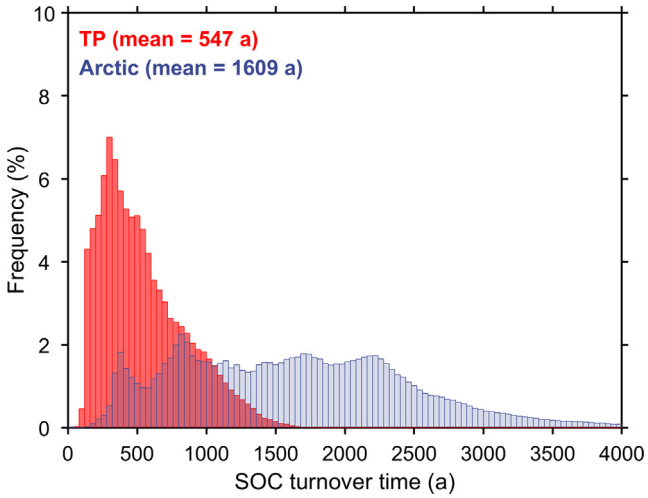

Fig. 3. Histograms of gridded topsoil organic carbon turnover times in TP grassland and Arctic tundra. The gridded turnover times (in years) in TP grassland and Arctic tundra are extrapolated from their own relationships between soil organic carbon (SOC) turnover times and environmental variables. Values in parentheses are regional-mean carbon turnover times that are calculated by averaging gridded values over TP grassland and Arctic tundra, respectively.

grassland. For Arctic tundra, soil carbon turnover times are longer in Eurasia than in Northern America (Fig. S20 online). On regional scale, the mean soil carbon turnover time (1609^{2181}_{1223} years) over Arctic tundra is about threefold as long as that in TP grassland (547^{575}_{520} years) (Figs. 3, S21 and S22 online). Our results thus indicate that soil carbon turnover time primarily accounted for the large differences in topsoil organic carbon density between the two regions.

3.4. Possible mechanisms for the different carbon turnover times

First, TP grassland (MAT = −3.5 °C) have a warmer climate than Arctic tundra (MAT = −9.9 °C) (Fig. S12 online). The relatively warmer conditions would be expected to enhance SOC decomposition rates and reduce the soil carbon turnover time. To diagnose whether such a difference in MAT could mainly explain the difference in turnover times between the two regions, we compared the turnover times of TP grassland and Arctic tundra that fell into the same MAT and MAP bins in a climate space. However, we still observed a shorter turnover time over TP grassland than Arctic tundra in ~70% of the same MAT-MAP bins (Figs. 4 and S23 online). These results suggest that the climatic difference between the two regions cannot fully explain the turnover time difference between the two regions.

Second, there is clear evidence that nutrient availability is a key factor determining the SOC decomposition rate and therefore the turnover time [7,40]. To test this mechanism, we collated published soil organic matter C/N ratio data, a good indicator of soil nutrient status, and found that TP grassland has a lower value (9–12) [41] than does Arctic tundra (20–30) (Fig. S24 online) [42]. The larger C/N ratio of soil organic matter in Arctic tundra than in TP grassland may be related to the weaker biological nitrogen fixation [43] and lower nitrogen deposition [44]. When microbes feed on substrates that are poor in nutrients compared to their demands, microbial decomposition rates would be greatly

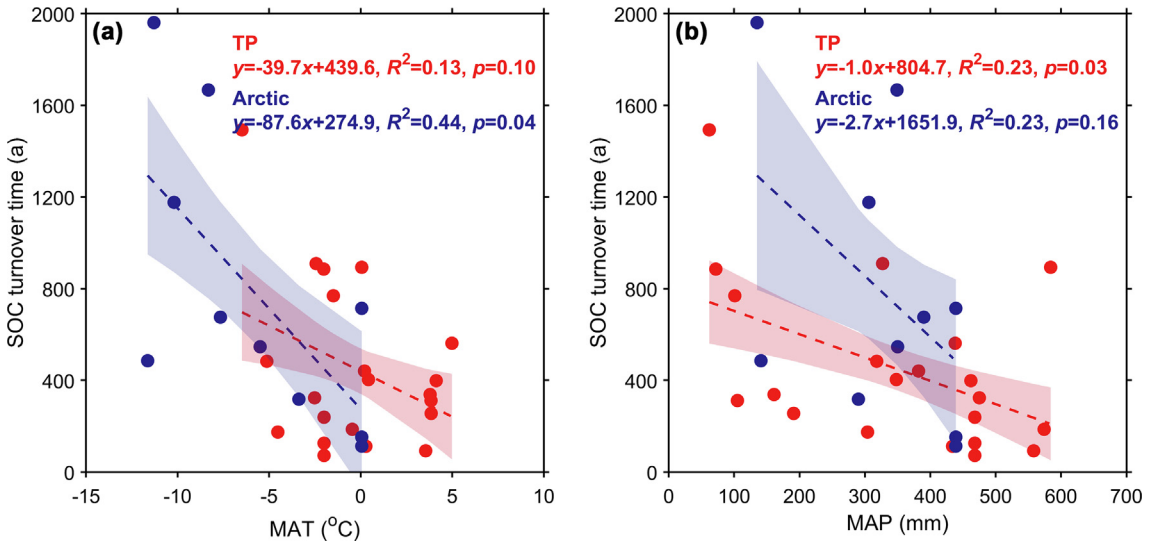

Fig. 2. Relationships between topsoil organic carbon turnover time and climate variables. (a) Relationships with mean annual temperature (MAT) in the TP grassland (red) and Arctic tundra (blue). (b) Mean annual precipitation (MAP) in the TP grassland (red) and Arctic tundra (blue). Here, carbon turnover times for all the sites were converted from observed ^{14}C data in topsoil (0–10 cm) with box model for a supposedly homogeneous reservoir.

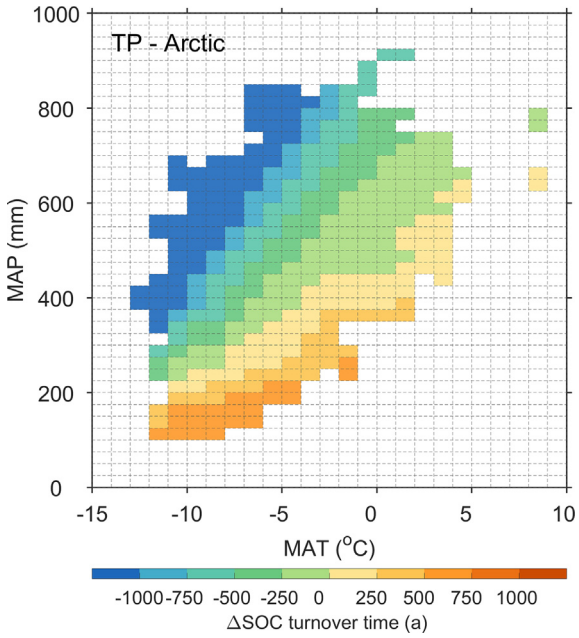

Fig. 4. Difference of topsoil organic carbon turnover times between TP grassland and Arctic tundra in the climate space. Difference of turnover times (△SOC turnover time, in years) is shown in each 1 °C interval of mean annual temperature (MAT) and 25-mm interval of mean annual precipitation (MAP) climate space. The MAT and MAP, which are calculated by averaging the period from 1970 to 2000, are derived from WorldClim Version 2.0 dataset.

restricted [45]. Such a nutrient limitation could occur in Arctic tundra due to a much higher C/N ratio in soil organic matter (20–30) than in microbes (7–13), and has a lower probability of occurring in TP grassland because the C/N ratios between microbes (10–15) and soil organic matter (9–12) are comparable there (Fig. S24 online). Such a limitation in the Arctic tundra would tend to slow the soil carbon decomposition rates and lengthen the turnover time, contributing to a longer turnover time in Arctic tundra than in TP grassland. In addition, the turnover time also generally increased with clay content, since this would tend to increase the stabilization of organic matter [46,47]. However, this effect did not constitute a possible explanation since clay content did not show any significant difference between the two regions (Fig. S14 online).

Third, photodegradation, the direct photochemical mineralization and indirect photofacilitation of organic matter mediated by sunlight (solar irradiance, specifically ultraviolet-B radiation), has been proposed as an important control of carbon turnover in water-limited ecosystems [48,49]. To test this hypothesis, we compared the solar radiation and ultraviolet-B radiation, which are important for the photodegradation of organic matter [50,51], between TP grassland and Arctic tundra. We found that the mean annual solar radiation (184 W m^{-2}) and ultraviolet-B radiation (0.065 W m^{-2}) in TP grassland were significantly higher than in Arctic tundra (105 and 0.014 W m^{-2}) (Fig. S13 online). This suggests that a stronger photodegradation impact on the carbon turnover occurs in TP grassland than in Arctic tundra, which may contribute to their faster carbon turnover.

Fourth, livestock grazing has a long history in TP grassland, and the impact of such human-induced grazing on ecosystems is more intense in TP grassland than in Arctic tundra. For example, human appropriation of net primary productivity, as a measure of human intervention into ecosystems [52], is much stronger in TP grassland (9.5%) than that in Arctic tundra (0.7%) (Fig. S25 online). Such intensified grazing might accelerate carbon decomposition rates and shorten the turnover time by shifting soil microbial composition from fungi-dominated to bacterial-dominated communities [53]. *Ad hoc* herbivore enclosure experiments will be needed to ascertain the importance of grazing on soil carbon turnover time in TP grassland [54].

4. Conclusion

In conclusion, our compilation of soil radiocarbon measurements showed that the soil carbon turnover time in the topsoil layer over TP grassland was about one-third as long as that in Arctic tundra, which mainly explains the observation that soil carbon density in TP grassland is less than a half of that in the Arctic tundra. The possible mechanisms behind the shorter turnover time in TP grassland proposed here are valid but qualitative, and require additional researches (e.g., field experiments) to quantify the processes [55]. In particular, there is a need for *ad hoc* experiments over TP grassland to elucidate the impact of grazing intensity and photodegradation on the turnover time. While the temperature control of soil carbon turnover is implicit for the two regions, precipitation is also found to be a key control in TP grassland, pointing out the need for a better understanding of changes in the monsoon-regulated hydrological cycle over TP grassland [56]. Our results highlight the diverse possible formation and stabilization mechanisms of soil organic carbon between the two vulnerable regions. We thus emphasize the necessity of representing heterogeneous carbon turnover in different permafrost zones and incorporating regional-specific mechanisms controlling the turnover in the land surface components of Earth System Models that can be used to understand the magnitude of carbon-climate feedback.

Conflict of interest

The authors declare that they have no conflict of interest.

Acknowledgments

This work was supported by Preliminary Research on Three Poles Environment and Climate Change (2019YFC1509103), the National Natural Science Foundation of China (41861134036 and 41922004), the Second Tibetan Plateau Scientific Expedition and Research Program (2019QZKK0606), and the Strategic Priority Research Program (A) of the Chinese Academy of Sciences (XDA19070303 and XDA20050101). We thank Susan Trumbore and James Randerson at Department of Earth System Science, University of California for providing the radiocarbon data in Arctic tundra.

Author contributions

Shilong Piao designed the research, Donghai Wu, Tao Wang and Shilong Piao wrote the paper, Donghai Wu and Dan Liu performed statistical analyses, Gengxin Zhang provided radiocarbon measurements over the Tibetan Plateau, and all authors contributed to the interpretation of results.

Appendix A. Supplementary materials

Supplementary materials to this article can be found online at https://doi.org/10.1016/j.scib.2021.04.019. The maps of topsoil organic carbon density, primary production and carbon turnover time for TP grassland and Arctic tundra can be downloaded from https://github.com/donghaiwu/DataShare.

References

[1] MacDougall AH, Avis CA, Weaver AJ. Significant contribution to climate warming from the permafrost carbon feedback. Nat Geosci 2012;5:719–21.
[2] Koven CD, Ringeval B, Friedlingstein P, et al. Permafrost carbon-climate feedbacks accelerate global warming. Proc Natl Acad Sci USA 2011;108:14769–74.
[3] Schuur EAG, McGuire AD, Schadel C, et al. Climate change and the permafrost carbon feedback. Nature 2015;520:171–9.
[4] Ding J, Li F, Yang G, et al. The permafrost carbon inventory on the Tibetan Plateau: a new evaluation using deep sediment cores. Glob Change Biol 2016;22:2688–701.
[5] Hugelius G, Tarnocai C, Broll G, et al. The northern circumpolar soil carbon database: spatially distributed datasets of soil coverage and soil carbon storage in the northern permafrost regions. Earth Syst Sci Data 2013;5:3–13.
[6] Post WM, Emanuel WR, Zinke PJ, et al. Soil carbon pools and world life zones. Nature 1982;298:156–9.
[7] Hobbie SE, Schimel JP, Trumbore SE, et al. Controls over carbon storage and turnover in high-latitude soils. Glob Change Biol 2000;6:196–210.
[8] Margesin R. Permafrost soils. Berlin: Springer; 2009.
[9] Yan Y, Zhou X, Jiang L, et al. Effects of carbon turnover time on terrestrial ecosystem carbon storage. Biogeosciences 2017;14:1–42.
[10] Friedl MA, Sulla-Menashe D, Tan B, et al. MODIS collection 5 global land cover: algorithm refinements and characterization of new datasets. Remote Sens Environ 2010;114:168–82.
[11] Todd-Brown K, Randerson J, Post W, et al. Causes of variation in soil carbon simulations from CMIP5 earth system models and comparison with observations. Biogeosciences 2013;10:1717–36.
[12] Hengl T, Mendes de Jesus J, Heuvelink GBM, et al. Soilgrids250m: global gridded soil information based on machine learning. PLoS One 2017;12:1–40.
[13] Batjes NH. Harmonized soil property values for broad-scale modelling (WISE30sec) with estimates of global soil carbon stocks. Geoderma 2016;269:61–8.
[14] Food and Agriculture Organization of the United Nations (FAO), International Institute for Applied Systems Analysis (IIASA), International Soil Reference and Information Centre World Soil Information (ISRIC), et al. Harmonized world soil database (version 1.2). FAO, Rome, Italy and IIASA, Laxenburg. Austria 2012:1–37.
[15] Jobbágy EG, Jackson RB. The vertical distribution of soil organic carbon and its relation to climate and vegetation. Ecol Appl 2000;10:423–36.
[16] Yang Y, Fang J, Guo D, et al. Vertical patterns of soil carbon, nitrogen and carbon: nitrogen stoichiometry in Tibetan grasslands. Biogeosci Discuss 2010;2010:1–24.
[17] Ding J, Chen L, Ji C, et al. Decadal soil carbon accumulation across Tibetan permafrost regions. Nat Geosci 2017;10:420–4.
[18] Jung M, Reichstein M, Margolis HA, et al. Global patterns of land-atmosphere fluxes of carbon dioxide, latent heat, and sensible heat derived from eddy covariance, satellite, and meteorological observations. J Geophys Res Biogeosci 2011;116:1–16.
[19] Yao Y, Wang X, Li Y, et al. Spatiotemporal pattern of gross primary productivity and its covariation with climate in China over the last thirty years. Glob Change Biol 2017;24:184–96.
[20] Bloom AA, Exbrayat J-F, van der Velde IR, et al. The decadal state of the terrestrial carbon cycle: global retrievals of terrestrial carbon allocation, pools, and residence times. Proc Natl Acad Sci USA 2016;113:1285–90.
[21] Xia J, Ma M, Liang T, et al. Estimates of grassland biomass and turnover time on the Tibetan Plateau. Environ Res Lett 2018;13:1–12.
[22] Yang Y, Fang J, Ma W, et al. Large-scale pattern of biomass partitioning across China's grasslands. Glob Ecol Biogeogr 2010;19:268–77.
[23] Raynolds MK, Walker DA, Epstein HE, et al. A new estimate of tundra-biome phytomass from trans-arctic field data and AVHRR NDVI. Remote Sens Lett 2012;3:403–11.
[24] Tucker CJ, Pinzon JE, Brown ME, et al. An extended AVHRR 8-km NDVI dataset compatible with MODIS and SPOT vegetation NDVI data. Int J Remote Sens 2005;26:4485–98.
[25] Oechel WC, Callaghan T, Gilmanov T, et al. Global change and arctic terrestrial ecosystems. New York: Springer; 2012.
[26] Yang Y, Fang J, Ji C, et al. Above- and belowground biomass allocation in Tibetan grasslands. J Veg Sci 2009;20:177–84.
[27] Jackson RB, Canadell J, Ehleringer JR, et al. A global analysis of root distributions for terrestrial biomes. Oecologia 1996;108:389–411.
[28] Fick SE, Hijmans RJ. Worldclim 2: new 1-km spatial resolution climate surfaces for global land areas. Int J Climatol 2017;37:4302–15.
[29] Beckmann M, Václavík T, Manceur AM, et al. Gluv: a global UV-B radiation data set for macroecological studies. Methods Ecol Evol 2014;5:372–83.
[30] Trumbore SE. Radiocarbon and soil carbon dynamics. Annu Rev Earth Planet Sci 2009;37:47–66.
[31] Tao Z, Shen C, Gao Q, et al. Soil organic carbon storage and soil CO_2 flux in the alpine meadow ecosystem. Sci China Ser D-Earth Sci 2007;50:1103–14.
[32] He Y, Trumbore SE, Torn MS, et al. Radiocarbon constraints imply reduced carbon uptake by soils during the 21st century. Science 2016;353:1419–24.
[33] Mathieu JA, Hatté C, Balesdent J, et al. Deep soil carbon dynamics are driven more by soil type than by climate: a worldwide meta-analysis of radiocarbon profiles. Glob Change Biol 2015;21:4278–92.
[34] Schuur EAG, Druffel ER, Trumbore SE. Radiocarbon and climate change. Switzerland: Springer International Publishing; 2016.
[35] Hua Q, Barbetti M, Rakowski AZ. Atmospheric radiocarbon for the period 1950–2010. Radiocarbon 2013;55:2059–72.
[36] Reimer PJ. IntCal13 and Marine13 radiocarbon age calibration curves 0–50000 years cal bp. Radiocarbon 2013;55:1869–87.
[37] Jackson RB, Lajtha K, Crow SE, et al. The ecology of soil carbon: pools, vulnerabilities, and biotic and abiotic controls. Annu Rev Ecol Evol Syst 2017;48:419–45.
[38] Cotrufo MF, Soong JL, Horton AJ, et al. Formation of soil organic matter via biochemical and physical pathways of litter mass loss. Nat Geosci 2015;8:776–9.
[39] Davidson EA, Janssens IA. Temperature sensitivity of soil carbon decomposition and feedbacks to climate change. Nature 2006;440:165–73.
[40] Sophie Z-B, Maria KK, Maria M, et al. The application of ecological stoichiometry to plant–microbial–soil organic matter transformations. Ecol Monogr 2015;85:133–55.
[41] Chen Y, Chen L, Peng Y, et al. Linking microbial C:N:P stoichiometry to microbial community and abiotic factors along a 3500-km grassland transect on the Tibetan Plateau. Glob Ecol Biogeogr 2016;25:1416–27.
[42] Xu X, Post WM. A global analysis of soil microbial biomass carbon, nitrogen and phosphorus in terrestrial ecosystems. Glob Ecol Biogeogr 2013;22:737–49.
[43] Davies-Barnard T, Friedlingstein P. The global distribution of biological nitrogen fixation in terrestrial natural ecosystems. Glob Biogeochem Cycles 2020;34:1–17.
[44] Galloway JN, Dentener FJ, Capone DG, et al. Nitrogen cycles: past, present, and future. Biogeochemistry 2004;70:153–226.
[45] He N, Yu G. Stoichiometrical regulation of soil organic matter decomposition and its temperature sensitivity. Ecol Evol 2016;6:620–7.
[46] Schmidt MWI, Torn MS, Abiven S, et al. Persistence of soil organic matter as an ecosystem property. Nature 2011;478:49–56.
[47] Schimel DS, Braswell BH, Holland EA, et al. Climatic, edaphic, and biotic controls over storage and turnover of carbon in soils. Glob Biogeochem Cycles 1994;8:279–93.
[48] Austin AT, Vivanco L. Plant litter decomposition in a semi-arid ecosystem controlled by photodegradation. Nature 2006;442:555–8.
[49] Susanna R, Davidi C, Dennis B, et al. Photodegradation leads to increased carbon dioxide losses from terrestrial organic matter. Glob Change Biol 2010;16:3065–74.
[50] Rozema J, Tosserams M, Nelissen HJM, et al. Stratospheric ozone reduction and ecosystem processes: enhanced UV-B radiation affects chemical quality and decomposition of leaves of the dune grassland species calamagrostis epigeios. Plant Ecol 1997;128:285–94.
[51] Thomasa D, Zhang E, Christophert R. Exposure to solar UV-B radiation accelerates mass and lignin loss of larrea tridentata litter in the sonoran desert. Plant Ecol 2007;193:185–94.
[52] Haberl H, Erb KH, Krausmann F, et al. Quantifying and mapping the human appropriation of net primary production in Earth's terrestrial ecosystems. Proc Natl Acad Sci USA 2007;104:12942–7.
[53] Xun W, Yan R, Ren Y, et al. Grazing-induced microbiome alterations drive soil organic carbon turnover and productivity in meadow steppe. Microbiome 2018;6:170.
[54] Sun J, Liu M, Fu B, et al. Reconsidering the efficiency of grazing exclusion using fences on the Tibetan Plateau. Sci Bull 2020;65:1405–14.
[55] Zhang Y, Zhu Y, Li J, et al. Current status and future directions of the Tibetan Plateau ecosystem research. Sci Bull 2019;64:428–30.
[56] Liu D, Wang T, Yang T, et al. Deciphering impacts of climate extremes on Tibetan grasslands in the last fifteen years. Sci Bull 2019;64:446–54.

Donghai Wu is currently a post-doctoral associate at the Department of Ecology and Evolutionary Biology, Cornell University, USA. He received the Ph.D. degree from the College of Urban and Environmental Sciences, Peking University, China in 2019. His research interest includes carbon turnover and ecosystem resilience.

Dan Liu is currently a postdoc at the Key Laboratory of Alpine Ecology, Institute of Tibetan Plateau Research, Chinese Academy of Sciences. She received her Ph.D. degree at Beijing Normal University in 2016. Her research focuses on the combined use of satellite data and models to understand carbon cycle in cold regions.

Gengxin Zhang is a professor at Institute of Tibetan Plateau Research, Chinese Academy of Sciences. His current research focuses on the response mechanism of soil microbial community and soil carbon pools dynamics to climate change in alpine ecosystem.

Shilong Piao is Cheung Kong Professor of Peking University. His current research focuses on the data model integration to improve our ability for predicting terrestrial ecosystem responses to global change.